A Jefferson Lab PAC 51 Letter of Intent

Nuclear Color Transparency via u-Channel Electproduction Observables

Wenliang (Bill) Li*

Center for Frontiers in Nuclear Science, Stony Brook, 11794, NY, USA and

Stony Brook University, Stony Brook, 11794, NY, USA

Garth Huber

University of Regina, Regina, SK, S4S0A2 Canada

Wim Cosyn

Florida International University, Miami, 33199, FL, USA

Bernard Pire

CPHT, CNRS, École Polytechnique, IP Paris, 91128-Palaiseau, France

(Dated: May 22, 2023)

The proposed measurement is a dedicated study to investigate the exclusive electroproduction process: γ^*+A$\rightarrow$(A-1)+p+π^0, where π^0 is produced via the u-channel process and the interacted proton (p) recoils forward with large momentum (leading). The measurement is designed to be above the nucleon resonance region with desired $W \sim 3$ GeV, which corresponds to $E_\gamma \sim 4$ GeV. The Hall C spectrometers (HMS+SHMS) under the standard configuration will tag the scattered electron (e') and recoiled proton in coincidence mode. The objective is to test the Color Transparency (CT) onset in the explored u-channel kinematics where a small transverse size proton is generated by the hard subprocess, and should therefore experience color ("half") transparency in its propagation through the nucleus.

* billlee@jlab.org

I. INTRODUCTION

Although a fundamental prediction of quantum chromodynamics (QCD) [1, 2], the phenomenon of color transparency (CT) has been, for many decades, a domain of controversial interpretations of experimental data; for a review, see ref. [3]. Together with scaling laws and polarization tests, the increase in nuclear transparency (NT) ratio with the relevant hard scale (denoted as Q^2) is believed to constitute an important signal of the onset of a collinear QCD factorization regime where hadrons transverse sizes shrink proportionally to $1/Q$, thus drastically diminishing final-state interaction cross-sections.

Near forward exclusive photon or meson electroproduction processes have been the subject of intense theoretical and experimental studies [4, 5]. Most of the available data are now interpreted in terms of a collinear QCD factorized amplitude, where generalized parton distributions (GPDs) are the relevant hadronic matrix elements. The study of nuclear transparency for meson electroproduction [6, 7] revealed a growth of the CT ratio, indicative of the early onset of the scaling regime. This may, however, appear to be contradictory to the non-dominance of the leading twist pion production amplitude revealed by the small value of the virtual photon's longitudinal-to-transverse structure function ratio σ_L/σ_T for this reaction [8, 9]. Alternative models have been proposed [10] to explain this fact.

The recent result from JLab experiment E12-06-17, presented in Fig. 1, ruled out the possibility of CT via the quasi-elastic $^{12}\mathrm{C}(e, e'p)$ reaction, which raised further questions on the transitioning to the perturbative QCD regime for this reaction. Of course, the community is eagerly waiting for the final results from the CT observation from the π^+ exclusive electroproduction reaction (from E12-06-17). At the same time, the authors of this proposal feel it is necessary to expand the current scope of CT studies into unexplored u-channel interaction kinematics.

Exclusive electroproduction processes in the complementary near backward region, where $-u = -(p_{\mathcal{M}} - p_N)^2 \ll Q^2$ (see definitions in Fig. 2), is near the minimal $-u$ value [11], should also be described at large Q^2 in a collinear QCD factorization scheme [12–14], where nucleon to meson transition distribution amplitudes (TDAs) replace the GPDs as the relevant hadronic matrix elements [15] and where the final state nucleon is described by its distribution amplitude (DA), i.e. as small transverse size ($O(1/Q)$) object. Observationally, the CT at the u-Channel kinematics under TDA interpretation unveils the unique and intriguing concept of "**half transparency**" (detailly described in Sec. III A). Indeed, the first experimental studies [16–18] of this new domain,

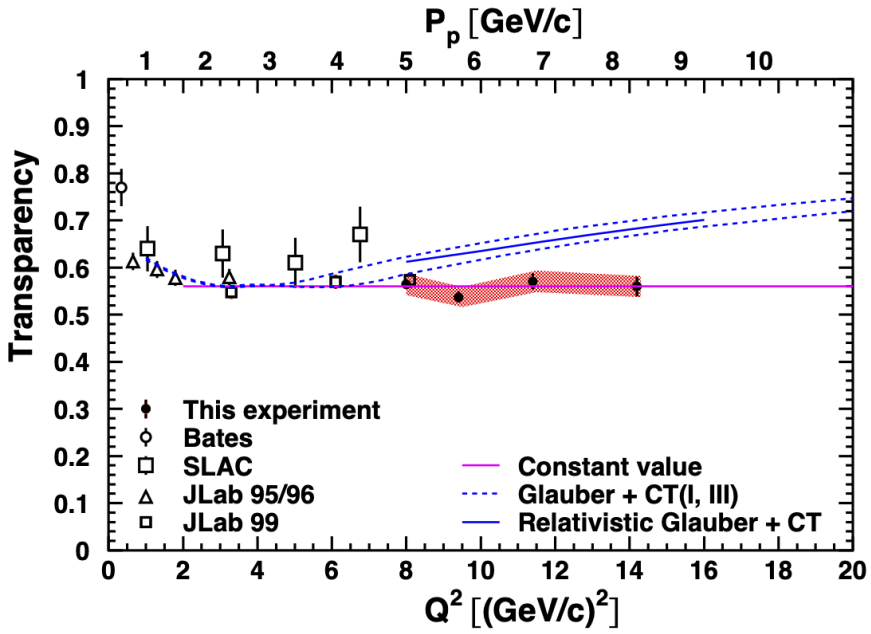

FIG. 1: The carbon nuclear transparency via quasi-elastic $^{12}C(e,e'p)$, reported by JLab E12-06-17 along with all previous experiments [19–23]. The Q^2 is shown along the x-axis (bottom scale), and the momentum of the knocked-out proton is also shown along the top scale of the x-axis. The solid magenta line is for a constant value of 0.56. The dashed lines are theory predictions including CT [24] for two different sets of parameters and the solid blue line is a prediction from a relativistic Glauber calculation with CT [25]. The error bars show the statistical uncertainty while the band shows the 4.0% systematic uncertainty. This plot was published in Ref. [26].

at rather moderate values of Q^2, point toward an early onset of the scaling regime.

This LoI is structured as follows: the evidence of early collinear factorization from the 6 GeV era is briefly summarised in Sec. II, along with the synergy with the approved 12 GeV program. Sec.III A elaborates the argument: why u-channel carries the potential to observe the CT onset and how the proposed measurement could serve as additional evidence to validate the TDA collinear factorization framework. The details of the proposed measurement and potential future follow at the upcoming Electron-Ion Collider (EIC) are covered in Sec. III C and III D.

II. PREVIOUS RESULTS AND SYNERGY WITH E12-20-007

The TDA collinear factorization framework has made two specific qualitative predictions regarding backward meson electroproduction in u-channel kinematics ($-u \to -u_{min}$ and correspondingly, $-t \to -t_{max}$), which can be verified experimentally [27, 28]:

- The characteristic $1/Q^8$-scaling behavior of the transverse cross-section for fixed x_B, fol-

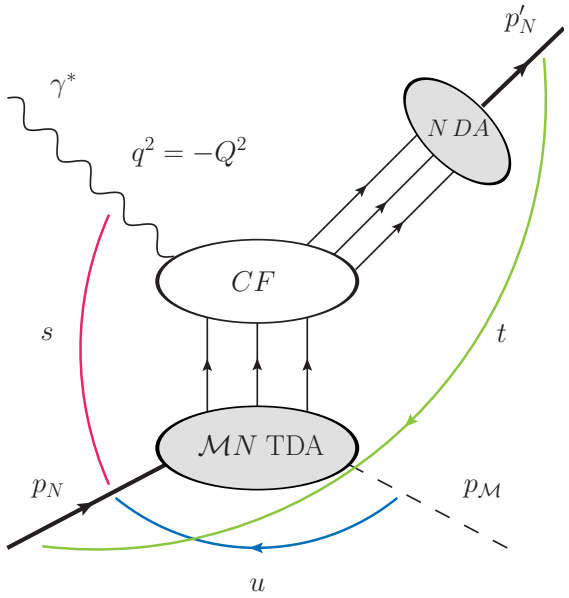

FIG. 2: Kinematical quantities and the collinear factorization mechanism for $\gamma^* N \to N\mathcal{M}$ in the near-backward kinematical regime (large virtuality Q^2, invariant mass W; fixed Bjorken x (or x_B); $|u| \sim 0$). q, p_N, $p_{\mathcal{M}}$, and p'_N are the four momenta of the virtual photon probe, initial state nucleon target, final state proton, and final state meson. The lower blob denoted $\mathcal{M}N$ TDA, depicts the nucleon-to-meson $\mathcal{M}$ transition distribution amplitude; the N DA blob depicts the nucleon distribution amplitude; CF denotes the hard subprocess amplitude (coefficient function). Here, s is the center-of-mass energy squared, and t and u denote the four-momentum differences squared (Mandelstam variables). These are defined as $s = W^2 = (q + p_N)^2$, $t = (p'_N - p_N)^2$, $u = (p_{\mathcal{M}} - p_N)^2$.

lowing the Q^2 behavior of the hard part of the process (namely $\gamma^* qqq \to qqq$).

- The dominance of the transverse polarization of the virtual-photon results in the suppression of the σ_L cross section by a least ($1/Q^2$): $\sigma_L/\sigma_T < 1/Q^2$.

In this section, we begin with a brief overview of the previous results on the u-channel exclusive meson electroproduction, which shows signs of early collinear factorization behavior in the Q^2 scaling in charged π^+ and $\sigma_L/\sigma_T \sim 0$ ratio in ω sector (Sec. II A. Sec. II B summarizes the upcoming experiment: E12-20-007, which is designed to simultaneously test both TDA predictions in the π^0 sector.

A. Previous Backward-Angle Data from JLab

The first data providing qualitative support for the TDA picture are from the JLab 6 GeV physics program [16–18].

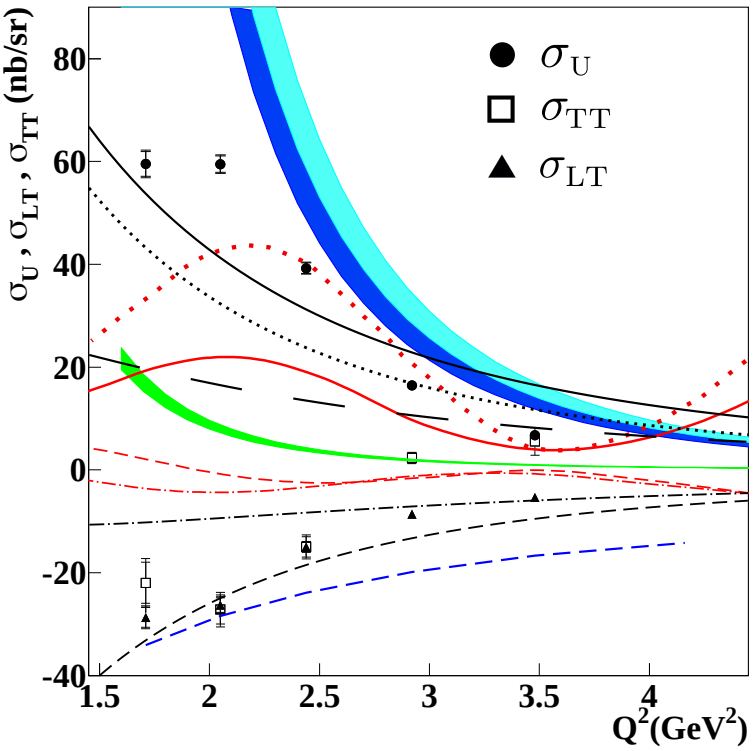

FIG. 3: The structure functions $\sigma_U = \sigma_T + \varepsilon\sigma_L$ (solid dot), σ_{TT} (square), and σ_{LT} (triangle) as a function of Q^2. ε describes the ratio between longitudinally and transversely polarized virtual photons, The inner error bars are statistical and the outer error bars are the combined systematic and statistical uncertainties in quadrature. The bands refer to model calculations of σ_U in the TDA description, green band: Braun-Lenz-Wittmann next-to-next-to-leading-order (BLW NNLO), dark blue band: Chernyak-Ogloblin-Zhitnitsky (COZ), and light blue band: King-Sachrajda (KS) (see [16] and Refs. therein for the meaning of these models). The lower blue short-dashed line represents an educated guess to fit the higher twist cross-sections σ_{LT} and σ_{TT} in the TDA picture. The red curves are the "Regge" predictions (by JML18) of [29, 30] for solid: σ_U, dashed curve: σ_{LT}, dot-dashed: σ_{TT}. An updated σ_U calculation from JML18 model [31] are shown in the red dotted curve. Regge calculations which consider parton contributions (see Ref. [32]) to σ_U, σ_T, σ_L, σ_{TT} and σ_{LT} are shown in black solid, black dotted, black long-dashed, black dot-dashed, and black short-dashed, respectively. This plot was recreated from the data and model predictions published in Refs. [16, 32].

Hard exclusive π^+ production ($ep \to e'n\pi^+$) from a polarized electron beam interacting with an unpolarized hydrogen target was studied with the CLAS detector in the backward angle kinematic regime by Park et al. [16]. Figure 3 shows the Q^2-dependence of $\sigma_U = \sigma_T + \varepsilon\sigma_L$, interference contributions σ_{LT} and σ_{TT}, obtained at the average kinematics of invariant mass $W = 2.2$ GeV and $-u = 0.5$ GeV^2 (defined in Figure 2 caption). ε describes the ratio of the fluxes of longitudinal and transverse virtual photons.

All three cross-sections have a strong Q^2 dependence. The TDA formalism predicts that the transverse amplitude dominates at large Q^2. With only this set of data at a fixed beam energy,

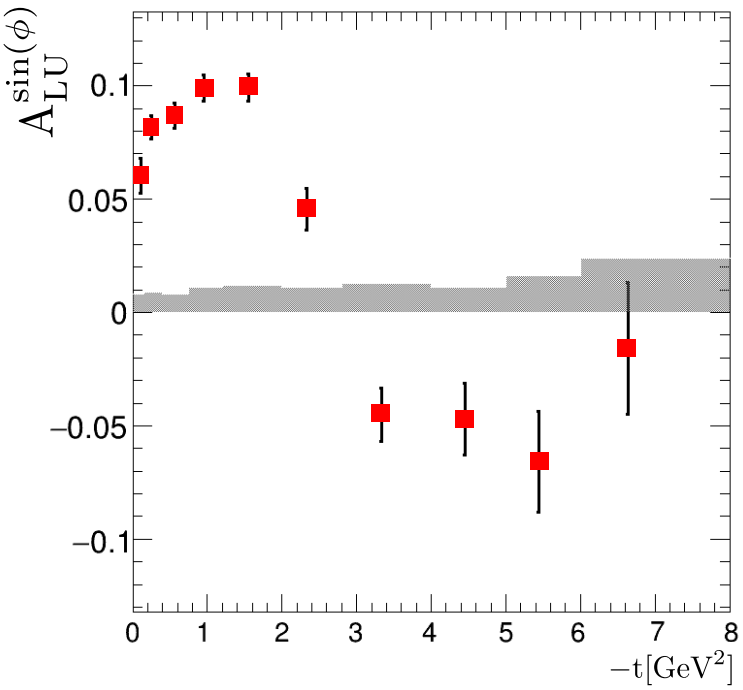

FIG. 4: Beam-spin asymmetry moment, $A_{LU}^{\sin\phi}$, as a function of $-t$ measured with CLAS at $W > 2$ GeV, $Q^2 > 1$ GeV^2. The maximal accessible value of $-t$ is ≈ 8.8 GeV^2. The shaded area represents systematic uncertainty. This plot was recreated from the data and model predictions published in Ref. [18].

the CLAS detector cannot experimentally separate σ_T and σ_L. After examining the angular dependence of σ_U, the results show σ_{TT} and σ_{LT} roughly equal in magnitude and with a similar Q^2-dependence. Their significant sizes (about 50% of σ_U) imply an important contribution of the transverse amplitude in the cross-section. Furthermore, above $Q^2 = 2.5$ GeV^2, the trend of σ_U is qualitatively consistent with the TDA calculation, yielding the characteristic $1/Q^8$ dependence expected when the backward collinear factorization scheme is approached.

The beam spin asymmetry moment, $A_{LU}^{\sin\phi}$, with ϕ being the azimuthal angle from the scattering plane, was also extracted using the CLAS detector [18]. $A_{LU}^{\sin\phi}$ is proportional to the polarized structure function $\sigma_{LT'}$,

$$A_{LU}^{\sin\phi} = \frac{\sqrt{2\varepsilon(1-\varepsilon)}\,\sigma_{LT'}}{\sigma_T + \varepsilon\sigma_L}, \tag{1}$$

where the structure functions σ_L and σ_T correspond to longitudinally and transversely polarized virtual photons.

Due to the large acceptance of CLAS, it was possible to map out the full kinematic region in

$-t$ (defined in Figure 2 caption) from very forward kinematics ($-t/Q^2 \ll 1$), where a description based on Generalized Parton Distributions (GPD) can be applied, up to very backward kinematics ($-u/Q^2 \ll 1$, $-t$ large), where a TDA-based description is expected to be valid. The results in Figure 4 indicate a transition from positive $A_{LU}^{\sin\phi}$ in the forward regime to rather small negative values in the backward regime, with a Q^2 dependence qualitatively consistent with the TDA picture. The sign change between the forward and backward kinematic regimes is independent of Q^2 and x_B within the kinematics accessible with CLAS.

Backward-angle exclusive ω electroproduction ($ep \rightarrow e'p\omega$) was studied in Hall C by Li et al. [17]. The scattered electron and forward-going proton was detected in the High Momentum Spectrometer (HMS) and Short Orbit Spectrometer (SOS), and the low-momentum rearward-going ω was reconstructed using the missing mass reconstruction technique. Since this method does not require the detection of the produced meson, it allows the analysis to extend the experimental kinematics coverage to a region that is inaccessible through the standard direct detection method.

The extracted $\sigma_{\rm L}$ and $\sigma_{\rm T}$, as a function of $-u$ at $Q^2 = 1.6$ and 2.45 GeV^2, are shown in Figure 5. The two sets of TDA predictions [33] for $\sigma_{\rm T}$ each assume different nucleon DAs [34, 35] as input. From the general trend, the TDA model offers a good description of the falling $\sigma_{\rm T}$ as a function of $-u$ at both Q^2 settings, similar to the backward-angle π^+ data from [16]. Together, the data sets are suggestive of early TDA scaling. The behavior of $\sigma_{\rm L}$ differs greatly at the two Q^2 settings. At Q^2 =1.6 GeV^2, $\sigma_{\rm L}$ falls almost exponentially as a function of $-u$; at Q^2 =2.45 GeV^2, $\sigma_{\rm L}$ is constant near zero (within one standard deviation). Note that the TDA model predicts a small-higher twist-$\sigma_{\rm L}$ contribution, which falls faster with Q^2 than the leading twist $\sigma_{\rm T}$ contribution.

B. Synergy with the Approved JLab Experiment E12-20-007

The first dedicated experiment for exclusive π^0 production in backward kinematics ($ep \rightarrow e'p\pi^0$), was proposed by Li, et al. in [36]. Here, the produced π^0 is emitted 180 degrees opposite to the virtual-photon momentum (at large momentum transfer), and is reconstructed via the missing mass technique, just as in [17]. This study aims to apply the Rosenbluth separation technique to provide model-independent L/T-separated differential cross-sections at the never explored u-channel kinematics region near ($-t = -t_{\rm max}$, $-u = -u_{\rm min}$).

The kinematic coverage of the experiment is shown in Figure 6. The L/T-separated cross-

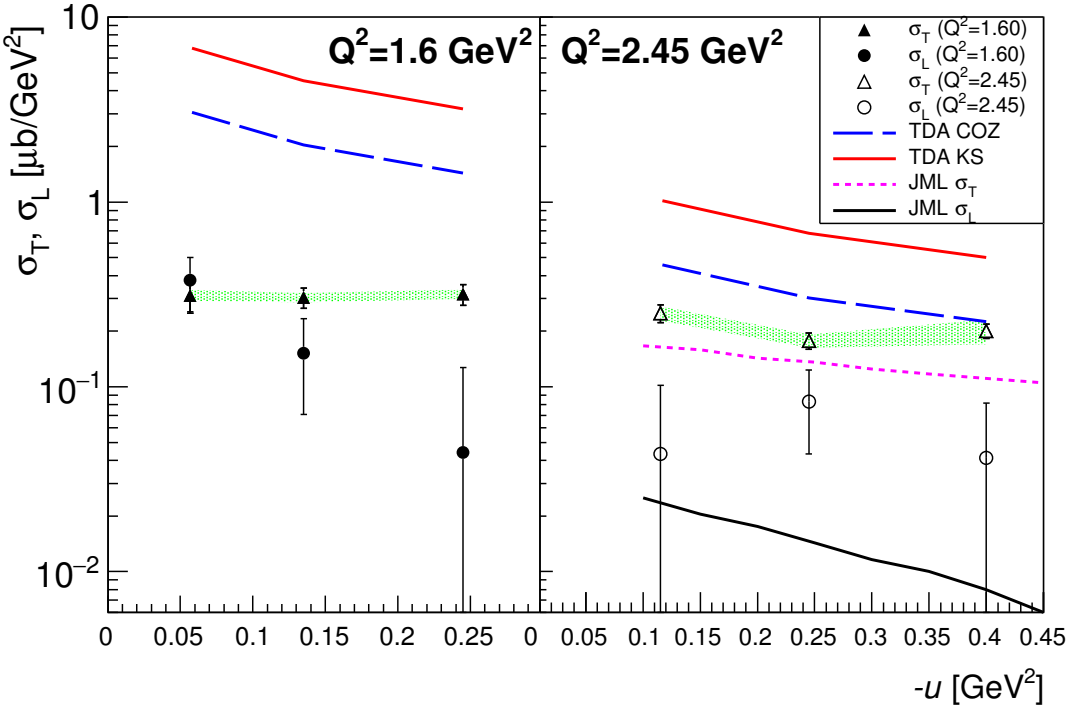

FIG. 5: σ_T (triangles), σ_L (squares) as a function of $-u$, at $Q^2 = 1.6$ GeV^2 (left), 2.45 GeV^2 (right). For the lowest $-u$ bin, $u' = u - u_{\rm min} \approx 0$. TDA predictions for σ_T: COZ (blue dashed lines), KS (red solid lines). The predictions were calculated at the specific $\overline{Q^2}$, $\overline{W}$ values of each u bin (overline represents the nominal value), and the predictions at three u bins joined by straight lines for visualization purposes. Green bands indicate correlated systematic uncertainties for σ_T, and the uncertainties for σ_L are similar. This plot was recreated from the data and model predictions published in Ref. [17].

sections are planned at $Q^2 = 2.0$, 3.0, 4.0, and 5.0 GeV^2. These measurements will provide the $-u$ dependence for $\sigma_{\rm L}$ and $\sigma_{\rm T}$ at nearly constant Q^2 and W, in addition to the behavior of $\sigma_{\rm L}/\sigma_{\rm T}$ ratio as function of Q^2. The $Q^2 = 6.25$ GeV^2 setting is chosen to test the Q^2 scaling nature of the unseparated cross-section, but only one ϵ setting is available due to limitations on the accessible spectrometer angles. These measurements are intended to provide a direct test of two predictions from the TDA model [37]: $\sigma_T \propto 1/Q^8$ and $\sigma_T \gg \sigma_L$ in u-channel kinematics. The magnitude and u-dependence of the separated cross-sections also provide direct connections to the re-scattering Regge picture [31]. The extracted interaction radius (from u-dependence) at different Q^2 can be used to study the soft–hard transition in the u-channel kinematics.

Relevant to this discussion is the definition of skewness. For forward-angle kinematics, in the regime where the handbag mechanism and GPD description may apply, the skewness is defined in

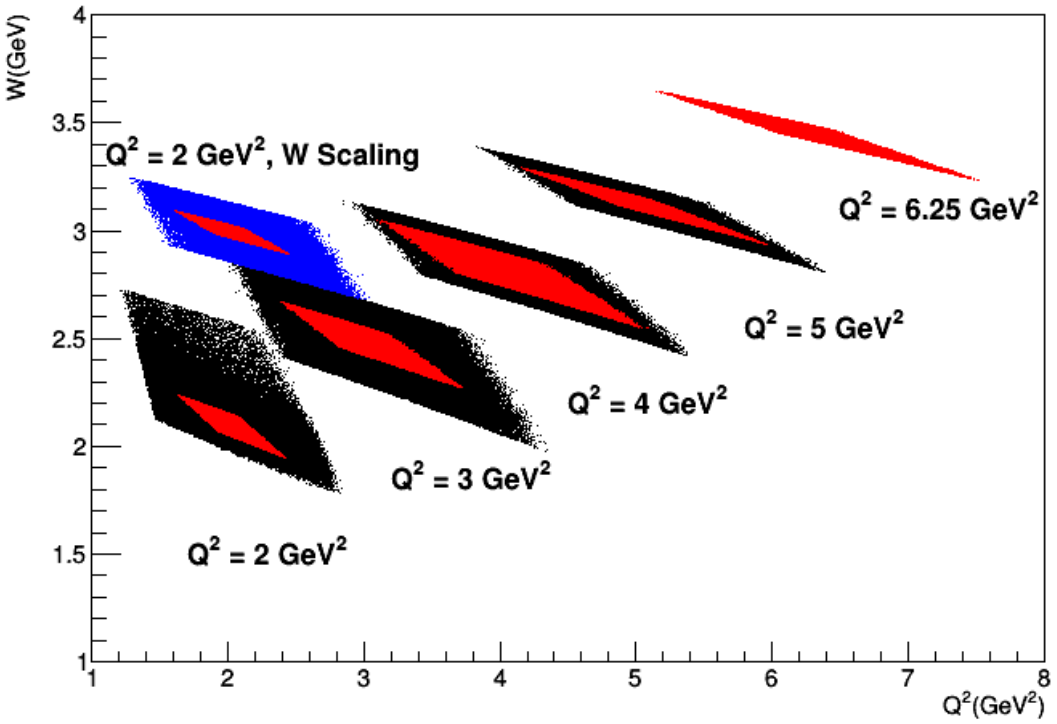

FIG. 6: W vs. Q^2 diamonds for the $Q^2 = 2.0$, 3.0, 4.0, 5.0, and 6.25 GeV^2 settings of the Jefferson Lab proposal E12-20-007. The black diamonds are for the higher ϵ settings and the red diamonds are for the lower ϵ settings. The diamonds for the W scaling setting are shown separately (in blue and red). Note that there is only one ϵ setting for $Q^2 = 6.25$ GeV^2. The overlap between the black and red diamond is critical for the L/T separation at each setting. The boundary of the low ϵ (red) data coverage will become a cut for the high ϵ data.

the usual manner,

$$\xi_t = \frac{p_1^+ - p_2^+}{p_1^+ + p_2^+}, \tag{2}$$

where p_1^+, p_2^+ refer to the light-cone plus components of the initial and final proton momenta [4]. The subscript t has been added to indicate that this skewness definition is typically used for forward-angle kinematics, where $-t \to -t_{\rm min}$. In this regime, ξ_t is related to x_B, and is approximated by $\xi_t = x/(2-x)$, up to corrections of order $t/Q^2 < 1$ [4]. This relation is an accurate estimate of ξ_t to the few percent for forward-angle electroproduction. In backward-angle kinematics, where $-t \to -t_{\rm max}$ and $-u \to -u_{\rm min}$, the skewness is defined with respect to u-channel momentum transfer in the TDA formalism [15],

$$\xi_u = \frac{p_1^+ - p_\pi^+}{p_1^+ + p_\pi^+}. \tag{3}$$

Figure 7 shows the forward ξ_t and backward ξ_u skewness coverage of the approved measurements. The "soft–hard transition" in u-channel meson production is an interesting and unexplored subject. The acquisition of these data will be an important step forward in validating the existence of a backward factorization scheme of the nucleon structure function and establishing its applicable kinematic range.

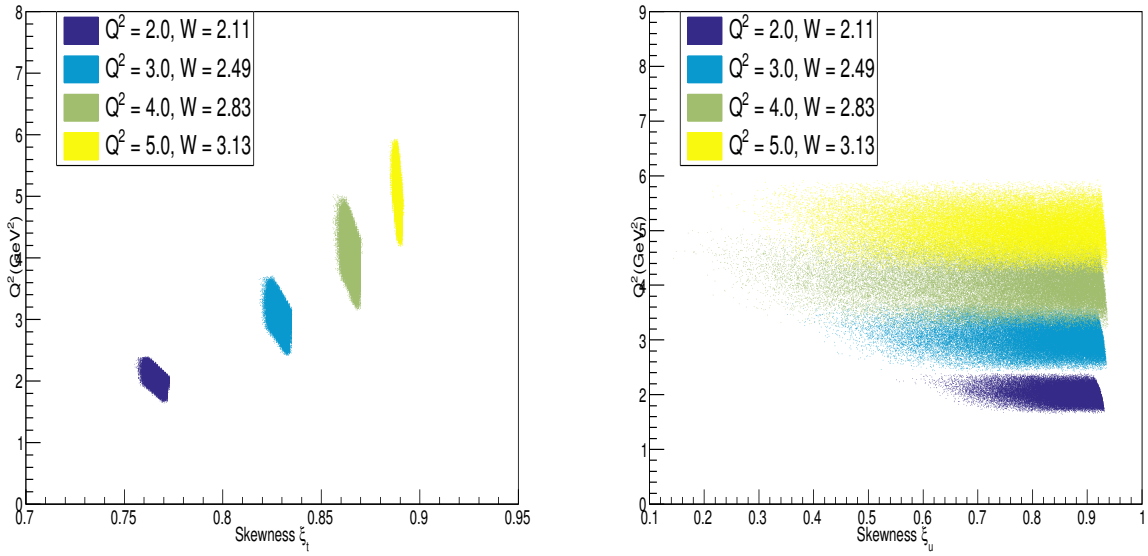

FIG. 7: Left: forward skewness ξ_t, Right: backward skewness ξ_u coverage of the planned E12-20-007 measurements for $Q^2 = 2.0$ to 5.5 GeV^2 (see text for definitions). Clearly, the experiment probes a wide kinematic range, which will be helpful for distinguishing the roles of the TDA and Regge reaction mechanisms in the soft–hard transition range.

III. THE PROPOSED MEASUREMENT

A. Question: Early Factorization in the u-Channel Kinematics?

The experimental data at JLab 6 GeV (described in Sec. II A) hint at the early onset of the QCD-based factorized description of electroproduction of mesons in the backward kinematics regime for Q^2 in the few GeV^2 range; this preliminary conclusion is drawn based on the qualitative agreement of data with the predictions of the collinear QCD description in terms of TDAs. However, the authors are conscious that the validation of the TDA framework requires further measurements (L/T separated cross-section) for all meson final states, where the two quantitative predictions need to be confirmed. This validation period is likely to last the entire phase JLab 12 GeV and the

proposed E12-20-007 is the first step of this process.

The authors of this LoI, while actively looking for new experimental observables to validate the collinear QCD description in the quite moderate Q^2 range currently accessed, **believe that the observation of CT in u-channel kinematics could serve as a third validation evidence to provide the claim of early factorization at backward angles.**. Indeed, $(e, e'p)$ measurements are a natural place to look for CT, and backward meson electroproduction on nuclei has to be subject to the color transparency phenomenon if the collinear QCD factorization framework applies. The observation of a clear CT signal would significantly shorten the validation period needed for the TDA framework. Following the TDA interpretation, the target proton would transition into a final state meson while emitting three quarks into the forward direction, which hadronize into another proton. Since the newly formed proton inherited only part of the target proton structure, therefore the CT observable of such interaction could describe the partial transparent nature of proton wavefunction, a.k.a the intriguing concept of "**half transparency**".

It is also worth noting that the EIC in its currently planned configuration will be able to perform the proposed measurement at higher $Q^2 > 6$ GeV^2, while high-quality measurements for $Q^2 < 6$ GeV^2 must be attempted at JLab.

B. Proposed measurement

Since the JLab 6 GeV backward-angle data are qualitatively consistent with early factorization in backward kinematics, backward-angle meson production events with a high momentum forward proton may provide an alternate means of probing color transparency.

Exclusive π^0 production is considered as an example reaction, based on the kinematics of E12-20-007 (Sec. II B), but the technique is in principle extendable also to vector meson production. In this case, the scattered electron would be detected in the HMS, and the high-momentum forward-going proton detected in the Super High Momentum Spectrometer (SHMS) of Hall C, with the meson reconstructed via the missing mass technique. Table I shows an example of kinematics (at JLab 12 GeV) for the described measurement. A comprehensive experiment should cover a range of nuclear targets, such as ^{1,2}H, ^{12}C, ^{27}Al, ^{63}Cu, and ^{197}Au, aiming to get broadly similar statistical uncertainties for all targets. The most likely scenario would be for an initial measurement on a target such as ^{12}C, followed by subsequent measurements on other targets, with kinematics chosen according to the observation, or not, of CT in the u-channel.

TABLE I: Possible kinematics for a backward angle color transparency experiment in Hall C of Jefferson Lab. The approximate momentum and the angle of the detected scattered electron and proton, and the undetected π^0 are shown along with the expected t, u ranges covered by the data. Note that the feasibility of performing the proposed study at $P_{HMS} = 7.3$ GeV required further study, and measurement at an alternative setting will not impact the significance of the proposed study.

$A(e,e'p)\pi^0$ Kinematics for $E_{\rm beam} = 10.6$ GeV, $W = 2$ GeV					
Q^2	e'	p	π^0	t	u
GeV^2	GeV/c, deg	GeV/c , deg	GeV/c , deg	GeV^2	GeV^2
3	7.3 , 11.3°	3.9–3.6 , 23°–30°	0.2–0.5 , 202°–95°	-5.7 to -5.2	+0.5 to -0.1
6	5.7 , 18.1°	5.6–5.2 , 19°–24°	0.1–0.5 , 196°–79°	-8.8 to -8.2	+0.6 to 0.0
10	3.6 , 29.7°	7.7–7.3 , 13°–16°	0.0–0.5 , 193°–61°	-12.8 to -12.1	+0.6 to -0.1

Based on the simulations performed for E12-20-007 [36], and the experience of the earlier π^+ Hall C nuclear transparency experiment [6], the main physics background within the spectrometer acceptance is expected to come from multi-pion production. The lower limit for the two-pion production phase-space is estimated to be $m^2_{\rm missing} \sim 0.06$ GeV^2 for a ^{1}H target. Due to Fermi smearing, the event reconstruction resolution will be somewhat worse for the data from heavier nuclei, but this effect can be included in the simulations used to optimize the experimental cuts to be used for each nuclear target. In [6], the estimated multi-pion background contamination was $<$0.4%, so it is reasonable to expect this contamination to be no larger than a few percent here. The contamination of higher mass mesons (such as η and ρ) should be negligible. The remaining physics background would come from virtual Compton scattering (VCS). Although the missing mass reconstruction resolution will not allow the π^0 and VCS channels to be separated, this contamination is also expected to be $<$1%. Thus, the Hall C standard equipment should allow high-quality u-channel data to be acquired from nuclear targets, and allow nuclear transparency to be studied in backward exclusive π^0 electroproduction.

Detailed simulations prior to the submission of a full experimental proposal, including estimates of the effects of Fermi momentum on the missing mass resolution, are planned. The model calculations in Sec. III C assume integration over both s- and p-shell knockout. If we are able to separate the shells experimentally, this would provide an additional lever in the CT study.

C. A Model Estimate of Nuclear Transparency

For the ^{12}C, ^{27}Al, ^{63}Cu, and ^{197}Au nuclei, estimates for the $A(e,e'p)\pi\, A-1$ nuclear transparency in the backward regime kinematics of Table I available in JLab Hall C are given here. These estimates are obtained using the relativistic multiple scattering Glauber approximation (RMSGA). The RMSGA is a flexible framework that treats kinematics and dynamics (nuclear wave functions, final-state interactions (FSI)) relativistically and has been applied to various hadron-, electron-, and neutrino-induced nuclear reactions; see [38–41] and references therein. The NT ratio is calculated as

$$T = \frac{\sigma^{\rm RMSGA}}{\sigma^{\rm PWIA}}\,, \tag{4}$$

where, in the calculation of the plane wave impulse approximation (PWIA) denominator, FSI is turned off and nominator and denominator are integrated over the experimentally accessible phase space. The cross-section is calculated in a factorized form [40]:

$$\frac{d\sigma^{eA}}{dE_{e'}d\Omega_{e'}dud\phi_N ds_2} = \int d\Omega^*_\pi \frac{m_{A-1}}{4s_2}\sqrt{\frac{\lambda(s_2,m_\pi,m_{A-1})\lambda(s_{\gamma N},m_N,-Q^2)}{\lambda(s_{\gamma A},m_A,-Q^2)}} \times \rho_D(p_i)\,\frac{d\sigma^{eN}}{dE_{e'}d\Omega_{e'}dud\phi_\pi}\,, \tag{5}$$

with integration over the solid angle of the (undetected) pion in the $(\pi, A-1)$ center-of-mass system. In the above equation, $u=(q-p_N)^2$, and the function,

$$\lambda(s,m_1,m_2) = [s-(m_1-m_2)^2][s-(m_1+m_2)^2] \tag{6}$$

was used. Here, the invariant masses squared $s=(p_\pi+p_{A-1})^2$, $s_{\gamma N}=(q+p_i)^2$, $s_{\gamma A}=(q+p_A)^2$, are introduced where p_N, p_π and p_{A-1} are the four-momenta of the final state proton, pion, and remnant $A-1$ nucleus, and

$$p_i = p_N + p_\pi - q \tag{7}$$

is the four-momentum of the initially struck nucleon. The nuclear initial state enters the distorted momentum distribution,

$$\rho_D(p_i) \equiv \sum_{m_s,\alpha_1} |\bar{u}(p_i,m_s)\phi^D_{\alpha_1}(p_i)|^2\,, \tag{8}$$

where the sum over α_1 runs over the quantum numbers of the occupied mean-field single-particle levels of the initial nucleus A. Here, m_s is the spin quantum number of the free spinor. The Dirac spinor wave functions $\phi^D_{\alpha_1}$ include the effects of the FSI between the detected nucleon and the remnant $A-1$ nucleus:

$$\phi^D_{\alpha_1}(p) = \frac{1}{(2\pi)^{3/2}} \int d^3r \; e^{-ip\cdot r} \; \phi_{\alpha_1}(r) \mathcal{F}^{\text{FSI}}(r) \, . \tag{9}$$

The FSI entering in $\mathcal{F}^{\text{FSI}}(r)$ are parametrized using nucleon-nucleon scattering data; see [40] for details. In the PWIA calculation, $\mathcal{F}^{\text{FSI}}(r) \to 1$ is set. The CT effects are implemented through the color diffusion model [42, 43], using $\Delta M^2 = 1.1$ GeV^2 in the nucleon coherence length $l_h = 2p_N/\Delta M^2$. The last ingredient of Equation (5) is the pion production cross-section on the nucleon, σ^{eN}, which was parameterized in the backward kinematics by interpolating the estimates provided in Ref. [36] (see Figure 19 and Appendix A therein), based on the model of Ref. [37].

Figure 8 shows the results of our calculations, where the central values from Table I are taken for the final state electron and proton kinematics. The transparency values lie in the expected range known from $A(e,e'p)$ calculations. The non-flat behavior of the regular Glauber (RMSGA) curve is due to the relative weight of s- and p- shell knockout differing between the considered points (central kinematics only). These estimates show that the proposed experiment should be able to distinguish color transparency effects. Note that these predictions can be further improved with a detailed Monte Carlo simulation study and can be extended to EIC kinematics.

D. Electron-Ion Collider Perspective on u-Channel eA Scattering

Despite the difference in the configuration compared to the JLab 12 GeV fixed target experiment, the future EIC [44–46] can be used to probe u-channel CT via meson electroproduction: $e+p \to e'+p'+\pi^0$ and $e+A(Z) \to e'+p'+A'(Z-1)+\pi^0$, where Z is the atomic number of the ion A beam. To directly extend the kinematics coverage (in Q^2) of the JLab measurement, the preferred beam scattering configuration requires a 5 GeV electron beam to collide with a 100 GeV per nucleon ion beam. It is important to note that EIC will offer a variety of ion beams, see details in Ref. [47]. The proposed measurement utilizes the electron and hadron end-caps, and integrated instrumentation in the far forward region (downstream of the outgoing ion beamline). The detection scenario is the following: the scattered electron will be captured by the electron end-cap; the

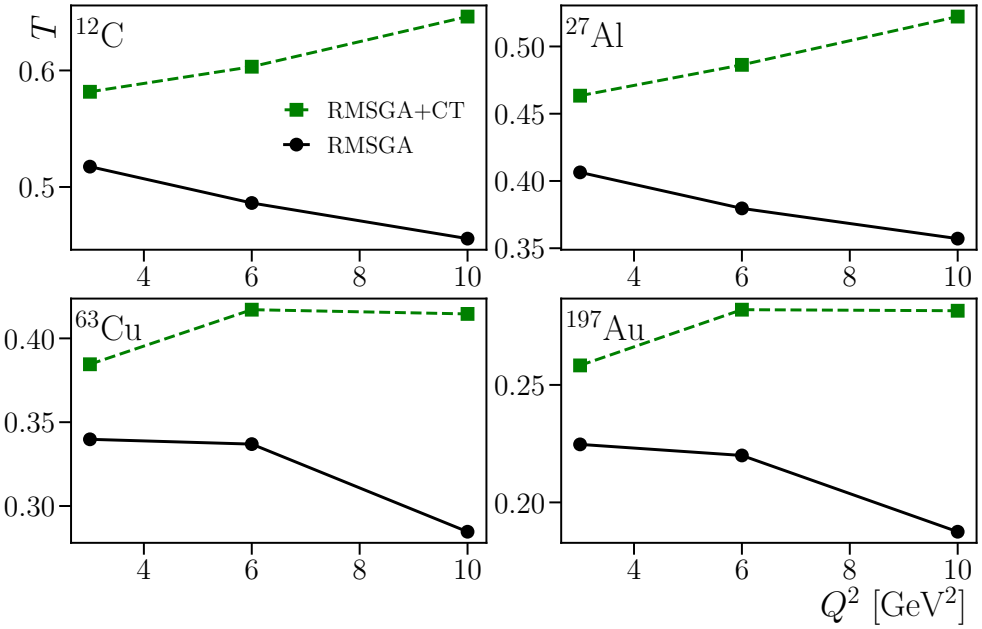

FIG. 8: RMSGA nuclear transparency calculations for ^{12}C, ^{27}Al, ^{63}Cu, and ^{197}Au as a function of Q^2. Full curves are regular Glauber calculations, the dashed curves include the color transparency in the quantum diffusion model.

induced virtual photon interacts with a nucleon within the nucleus, then the interacted nucleon transitions into a final state π^0 through TDA (in u-channel kinematics, see Figure 2); the fast proton (knocked out of the nucleus) will be picked up by the hadron end-cap and create a "start" in the timing window; the π^0 moves out of the nucleus and decays into two photons, thus projecting a one or two-photon signal in the far forward B0 or Zero Degree Calorimeter. In the case of eA scattering, the $A(Z)$ loses a proton due to the interaction and becomes $A'(Z-1)$, and can be captured by the Roman Pot detector due to the loss of total momentum and magnetic field steering. The feasibility of such a measurement is currently being studied by the EIC Comprehensive Chromodynamics Experiment (ECCE) consortium.

Here, it is important to point out that the color transparency study has been proposed at the EIC through $e+p$ and $e+A$ scatterings, and photoproduction of mesons [46, 48]. These CT studies are based on the validity of the collinear factorization theme in the small $-t$ kinematics and should be distinguished from the u-channel meson electroproduction observable proposed in this paper. In the former case, the final state meson will be produced by the $e+p$, and $e+A$ interactions and will be detected by the central barrel of the EIC; in the latter case, the interacted ion beam and the newly produced meson will both enter the far forward region, as described above.

IV. CONCLUDING REMARKS

The available data on nuclear transparency lead to the obvious conclusion that the phenomenon of color transparency (CT) needs to be further explored. This is particularly important for the nucleon case. The historical measurement [49] of the large angle proton-proton (pp) elastic and quasi-elastic$(p, 2p)$ scattering have led to many debates and interpretations [42, 50–52].

The $(e, e'p)$ measurements are a natural place to look for proton color transparency. The recent data on the $(e, e'p)$ reaction [26] demonstrated the absence of any positive signal for the manifestation of color transparency in this simple reaction up to $Q^2 = 14$ GeV^2, reinforcing doubts on the leading twist dominance of the nucleon form factors at experimentally available energy (especially at JLab 12 GeV). With transparency measurements available so far in a limited set of reactions and kinematics, it is too early to tell what drives the absence of the onset of CT in the proton case, while for forward meson production the onset has been observed.

Planned measurements at JLab will extend the known meson production processes to the maximum Q^2 values available using the 12 GeV beam at JLab. In this LOI, a complement to this existing color transparency program is described which expands the study to an unexplored territory of u-channel kinematics ($t \to t_{\max}$).

For the first time, we propose to link CT studies to backward meson electroproduction on nuclei, which are described in the collinear QCD factorization framework at sufficiently high Q^2. Contrary to the forward deep electroproduction of mesons process, where the fast forward going particle is a meson expected to experience CT, the backward process produces a fast nucleon. It should experience CT if it is born from a short distance process (technically speaking, if the hadronization occurs through its distribution amplitude convoluted to a hard partonic process), as is the case in the understanding of hard backward electroproduction in the colinear QCD factorization formalism, where transition distribution amplitudes (TDA) appear. Observation of CT will help to settle the controversy on the early scaling of exclusive reactions involving nucleons, by answering the question: does the exclusive meson electroproduction experiment witness the dominance of a small nucleon configuration in the backward kinematics where the nucleon has a large energy?

In a similar line of thought to this proposal, one may study nuclear transparency in various experiments (see [53]), where TDAs appear as the collinear factorized hadronic matrix element, while a hard scattering process should be accompanied by the appearance of color transparency. This is the case for timelike Compton scattering with a quasi-real photon beam [54], but also in

the antiproton nucleus electromagnetic processes at PANDA experiment [55] and the π-nucleus program at J-PARC [56]. In these three cases, color transparency should act as a decrease in the initial (rather than final) state interactions.

Once the proposed measurement is completed, a broader discussion within the community is necessary to determine the implication and the global significance of the observed experimental facts, i.e., validation of the TDA formalism, presence or absence of an onset of CT.

---

[1] A. H. Mueller, in *17th Rencontres de Moriond on Elementary Particle Physics: I. Electroweak Interactions and Grand Unified Theories* (1982), pp. 13–43.

[2] S. J. Brodsky, in *XIII International Symposium on Multiparticle Dynamics* (1982), pp. 963–1002.

[3] P. Jain, B. Pire, and J. P. Ralston, Physics Reports **271**, 67 (1996), ISSN 0370-1573, URL https://www.sciencedirect.com/science/article/pii/0370157395000712.

[4] M. Diehl, Phys. Rept. **388**, 41 (2003), ISSN 0370-1573, URL https://www.sciencedirect.com/science/article/pii/S0370157303003338.

[5] K. Kumericki, S. Liuti, and H. Moutarde, Eur. Phys. J. A **52**, 157 (2016).

[6] B. Clasie et al., Phys. Rev. Lett. **99**, 242502 (2007), 0707.1481.

[7] L. El Fassi et al. (CLAS), Phys. Lett. B **712**, 326 (2012), 1201.2735.

[8] M. Defurne et al. (Jefferson Lab Hall A), Phys. Rev. Lett. **117**, 262001 (2016), 1608.01003.

[9] M. Dlamini et al. (Jefferson Lab Hall A), Phys. Rev. Lett. **127**, 152301 (2021), 2011.11125.

[10] M. M. Kaskulov and U. Mosel, Phys. Rev. C **81**, 045202 (2010), URL https://link.aps.org/doi/10.1103/PhysRevC.81.045202.

[11] C. A. Gayoso et al., Eur. Phys. J. A **57**, 342 (2021), 2107.06748.

[12] L. Frankfurt, P. Pobylitsa, M. V. Polyakov, and M. Strikman, Phys. Rev. D **60**, 014010 (1999).

[13] B. Pire and L. Szymanowski, Phys. Rev. D **71**, 111501 (2005).

[14] B. Pire and L. Szymanowski, Phys. Lett. B **622**, 83 (2005).

[15] B. Pire, K. Semenov-Tian-Shansky, and L. Szymanowski, Phys. Rept. **940**, 2185 (2021), 2103.01079.

[16] K. Park et al. (CLAS Collaboration), Phys. Lett. **B780**, 340 (2018).

[17] W. B. Li et al. (Jefferson Lab Fπ), Phys. Rev. Lett. **123**, 182501 (2019).

[18] S. Diehl et al. (CLAS Collaboration), Phys. Rev. Lett. **125**, 182001 (2020).

[19] N. C. R. Makins et al., Phys. Rev. Lett **72**, 1986 (1994).

[20] T. O'Neill et al., Physics Letters B **351**, 87 (1995), ISSN 0370-2693.

[21] D. Abbott et al., Phys. Rev. Lett. **80**, 5072 (1998), URL https://link.aps.org/doi/10.1103/PhysRevLett.80.5072.

[22] K. Garrow et al., Phys. Rev. C **66**, 044613 (2002), URL https://link.aps.org/doi/10.1103/PhysRevC.66.044613.

[23] F. Willeke and J. Beebe-Wang (2021), URL https://www.osti.gov/biblio/1765663.

[24] L. L. Frankfurt, E. J. Moniz, M. M. Sargsyan, and M. I. Strikman, Phys. Rev. C **51**, 3435 (1995), URL https://link.aps.org/doi/10.1103/PhysRevC.51.3435.

[25] W. Cosyn, M. C. Martínez, J. Ryckebusch, and B. V. Overmeire, Phys. Rev. C **74**, 062201 (2006), URL https://link.aps.org/doi/10.1103/PhysRevC.74.062201.

[26] D. Bhetuwal, J. Matter, H. Szumila-Vance, M. L. Kabir, D. Dutta, R. Ent, D. Abrams, Z. Ahmed, B. Aljawrneh, S. Alsalmi, et al. (Jefferson Lab Hall C Collaboration), Phys. Rev. Lett. **126**, 082301 (2021), URL https://link.aps.org/doi/10.1103/PhysRevLett.126.082301.

[27] B. Pire and L. Szymanowski, Phys. Rev. Lett. **115**, 092001 (2015).

[28] B. Pire, K. Semenov-Tian-Shansky, and L. Szymanowski, Phys. Rev. D **84**, 074014 (2011).

[29] M. Guidal, J.-M. Laget, and M. Vanderhaeghen, Physics Letters B **400**, 6 (1997), ISSN 0370-2693, URL https://www.sciencedirect.com/science/article/pii/S0370269397003547.

[30] J.-M. Laget, Progress in Particle and Nuclear Physics **111**, 103737 (2020), ISSN 0146-6410.

[31] J. M. Laget, Phys. Rev. C **104**, 025202 (2021), 2104.13078.

[32] C. Ayerbe Gayoso et al. (2021), arXiv:2107.06748 [hep-ph].

[33] B. Pire, K. Semenov-Tian-Shansky, and L. Szymanowski, Phys. Rev. D **91**, 094006 (2015), 1503.02012.

[34] V. L. Chernyak, A. A. Ogloblin, and I. R. Zhitnitsky, Yad. Fiz. **48**, 1398 (1988).

[35] I. King and C. T. Sachrajda, Nucl. Phys. B **279**, 785 (1987).

[36] W. B. Li et al. (2020), 2008.10768.

[37] J. Lansberg, B. Pire, K. Semenov-Tian-Shansky, and L. Szymanowski, Phys. Rev. D **85**, 054021 (2012).

[38] J. Ryckebusch, D. Debruyne, P. Lava, S. Janssen, B. Van Overmeire, and T. Van Cauteren, Nucl. Phys. A **728**, 226 (2003), nucl-th/0305066.

[39] M. C. Martinez, P. Lava, N. Jachowicz, J. Ryckebusch, K. Vantournhout, and J. M. Udias, Phys. Rev.

C **73**, 024607 (2006), nucl-th/0505008.

[40] W. Cosyn, M. C. Martinez, and J. Ryckebusch, Phys. Rev. C **77**, 034602 (2008), 0710.4837.

[41] W. Cosyn and J. Ryckebusch, Phys. Rev. C **87**, 064608 (2013), 1301.1904.

[42] G. R. Farrar, H. Liu, L. L. Frankfurt, and M. I. Strikman, Phys. Rev. Lett. **61**, 686 (1988), URL https://link.aps.org/doi/10.1103/PhysRevLett.61.686.

[43] L. L. Frankfurt, W. R. Greenberg, G. A. Miller, M. M. Sargsian, and M. I. Strikman, Z. Phys. A **352**, 97 (1995), nucl-th/9501009.

[44] A. Accardi et al., Eur. Phys. J. **A52**, 268 (2016).

[45] E. Aschenauer, A. Kiselev, R. Petti, and T. Ullrich (2019).

[46] R. Abdul Khalek et al. (2021), arXiv: 2103.05419 [physics.ins-det].

[47] F. Willeke and J. Beebe-Wang (2021), URL https://www.osti.gov/biblio/1765663.

[48] F. Hauenstein et al. (2021), arXiv:2109.09509 [physics.ins-det].

[49] A. S. Carroll et al., Phys. Rev. Lett. **61**, 1698 (1988).

[50] S. J. Brodsky and G. F. de Teramond, Phys. Rev. Lett. **60**, 1924 (1988).

[51] J. P. Ralston and B. Pire, Phys. Rev. Lett. **61**, 1823 (1988).

[52] T. S. H. Lee and G. A. Miller, Phys. Rev. C **45**, 1863 (1992).

[53] P. Jain, B. Pire, and J. P. Ralston, in *The Future of Color Transparency and Hadronization Studies at Jefferson Lab and Beyond* (2022), 2203.02579.

[54] B. Pire, K. M. Semenov-Tian-Shansky, A. A. Shaikhutdinova, and L. Szymanowski (2022), 2201.12853.

[55] J. Lansberg, B. Pire, K. Semenov-Tian-Shansky, and L. Szymanowski, Phys. Rev. D **86**, 114033 (2012), [Erratum: Phys.Rev.D 87, 059902 (2013)].

[56] B. Pire, K. Semenov-Tian-Shansky, and L. Szymanowski, Phys. Rev. D **95**, 034021 (2017).